2019 SCEC Project Report

Is topography part of the "key" in the Cajon Pass earthquake gate?

Christodoulos Kyriakopoulos
Center for Earthquake Research and Information (CERI)
University of Memphis

David D. Oglesby (not funded in this proposal)
Department of Earth Sciences
University of California, Riverside

Amount funded: $30,000.00; (University of Memphis)

Proposal Category: B

SCEC Research Priorities / Science Objectives: 4a, 1e, 2e

Start Date: February 1, 2019

Abstract

The Cajon Pass (CP) is a key area for the generation of large earthquakes in southern California (SoCAL) and more specifically is thought to be an "Earthquake Gate" (EG). The mechanisms for which the CP serves as an EG are net yet understood and is of great importance to identify first order effects that modulate and control the generation of region-wide ruptures. In this work we are investigating whether the asymmetric topographic relief surrounding the CP could have an effect to this "gate-like" behavior. To do that we are using full 3D dynamic rupture models and comparing results between models with topography and models with a flat free surface. In our preliminary results, based on approximately 20 simulations, we observe a distinct pattern of normal stress change (not observed in the flat models) around the rupture front near the free surface. For example, in models with nucleation south of the CP (here the topography lies to the right of the fault), the rupture front is preceded by an increase in normal stress (clamping - blue color) and followed by a concentration of decreasing normal stress (unclamping – red color). When rupture passes the CP (topography now lies to the left of the fault) the normal stress pattern is inverted. The same pattern and pattern inversion are observed when rupture nucleates to the north of the CP and propagates southward. These preliminary results show that the CP marks a transition for rupture behavior and that this transition is (at least partially) related to the asymmetric disposition of the topographic relief.

1.Introduction and background

In southern California the San Andreas fault traverses or borders several topographic features that include deserts and high mountain reliefs. In the vicinity of the CP, the fault extends from the flat Coachella Valley to the base of the San Bernardino Mountains (3000+ m), runs through the Cajon pass and up into the San Gabriel Mountains, where it reaches an elevation of around 2000 m before descending down to the Mojave desert (**Figure 1**).Of particular interest in our investigation is the effect of the asymmetric disposition of the topography as the fault extends across the CP. More specifically, south of the CP the high topography (San Bernardino Mountains) is to the north of the SAF while once the fault passes the CP this relation is inverted and the high topography (San Gabriels Mountains) is to the south of the fault. In the past year we started investigating the effect that topography has on the rupture propagation and slip across the CP. We did that by using 3D dynamic rupture models and comparing results between models with topography and models with a flat free surface. Both types of models (flat and topographic) implement the southern San Andreas fault as described in UCERF3 (Field et al., 2013), including its nonplanar geometry. Our curiosity to investigate the topographic effect near the CP is supported by past and more recent findings. Previous work (e.g., Bouchon, 1973, Trifunac, 1973, Wong, 1982, Geli et al., 1988, Bouchon et al., 1996) investigated the effect of topography on wave propagation and specifically ground motion. Their results show that the interaction (scattering) of seismic waves with the irregular topographic surface produces significant frequency depended amplification or de-amplification phenomena. This interaction depends on the relative topographic wavelength. In the specific case of SoCAL, Ma et al., 2007 used wave propagation large scale modelling and investigated the effect of the San Gabriels Mountains on wave propagation. Their results show that the presence of the mountain range produces scattering and breaking up of the seismic waves. For that reason, the mountains "shield" the metropolitan area of Los Angeles and decrease the efficiency of damaging waves within the LA basin. Although the above works present important results regarding the interaction between propagating wave fronts and the irregular topographic surface (mountains and valleys), they do not explore the effect that

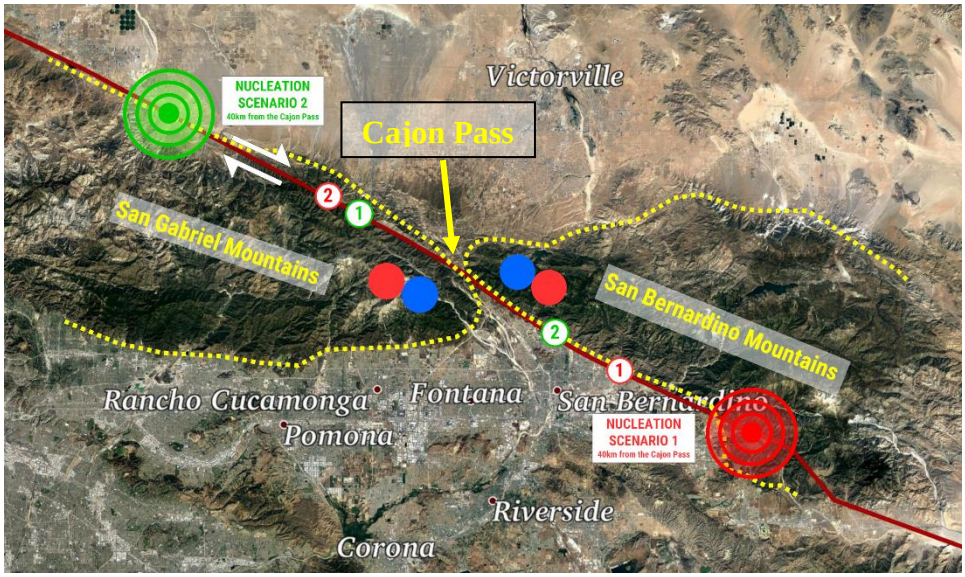

Figure 1. Google Earth Map of Southern California with regional topographic features. *The San Andreas fault passes through the Cajon Pass. Note that the San Bernardino and San Gabriel mountains are placed asymmetrically with respect of the fault trace (red dotted line). The yellow dotted line highlights the edge of the two mountains near the Cajon Pass. The red and green concentric circles mark the nucleation locations of our rupture scenarios, south and north of the Cajon pass respectively. The red and green numbers "1" and "2" show the observations points (time snapshots) used to investigate the normal stress changes in* ***Figure 3****. The red and blue solid circles show a schematic representation of the normal stress pattern observed in* ***Figure 3****.*

reflected waves have on the actual fault surface and propagation of rupture. In that prospective, a very limited number of studies exist, and their results imply that the effect of scattered reflections off the topography can have a significant effect on rupture propagation, specifically slip-rate and slip. Ely et al., 2010, compared results from flat and topographic dynamic rupture models that included the topography of the San Bernardino Mountains up to the CP. They noticed a burst of super shear speed during the rupture propagation in the topographic model, not detected in the equivalent dynamic rupture model with flat free surface. This work, although it includes the San Gabriel Mountains, it does not extend north of the CP, and for that reason does not investigate the asymmetric disposition of the topography. In a more recent work regarding the 2010 El Mayor-Cucapah earthquake, Kyriakopoulos et al. (2017) performed dynamic rupture simulations with a model implementing the Sierra del Los Cucapah mountain range and surrounding topography and compared these results with equivalent experiments using a flat free surface. They found noticeable differences between the two models, including the generation of higher and lower fault slip rates as well at times breaking up the coherence of the rupture front. Finally, Zhang et al., (2015) used dynamic rupture models with synthetic topographic features and showed that depending on the nucleation location topography can change the speed of rupture with implications for the super-shear transition. In the next section we are presenting preliminary results from our SCEC-funded project. We performed dynamic rupture simulations based on a finite element model that implements the topography of Southern California centered around the CP area. We ran a series of experiments by varying three main parameters. The nucleation location, the pre-stress level and the locking depth. All the simulations with the topographic model are repeated using an equivalent flat surface model and the discussion of our results is based on the comparisons between these two sets of experiments (topographic vs flat).

2. Modelling the Topographic Asymmetry near the Cajon Pass

A straightforward way to investigate the topographic effect is to compare results between dynamic rupture models with flat and topographic free surfaces. The finite element models used in this work were generated using the meshing code Trelis (csimsoft.com). The topographic layer was extracted using the GeoMapApp (.org) application and downsampled before the implementation in the mesh. Both the "flat" and "topographic" models implement the southern portion of the San Andreas fault as described in UCERF3 (Field et al., 2013). The total dimensions of the model domain are L220 km x W220 km x D50 km. To ensure the correct calculations of the stresses we generated a mesh with higher density (250m) around the fault interface that becomes three times larger (750m) outside the high-density volume. The final model is composed by approximately 30 million hexahedral elements. A more detailed description of the mesh is available in the 2018 proposal (SCEC #19223). We run our dynamic rupture scenarios using the finite element code FaultMod (Barall, 2009). FaultMod is extensively tested and benchmarked against other dynamic rupture codes within the SCEC benchmark exercise (Harris et al., 2009). In our simulations the allowed length of rupture is approximately 120 km along strike, with a 15 km locking depth. To isolate the first order effects of the topographic surface we chose to use homogeneous material properties with a Poisson ratio of 0.25, a V_P of 5477 m/sec, and a V_S of 3162 m/sec. We use slip-weakening friction (Ida, 1972; Andrews, 1976) with a static frictional value of 0.6, a sliding frictional value of 0.1, and a slip weakening distance of 0.3 m. To investigate the effect of topography we run several simulations by varying the nucleation location, the pre-stress level and the locking depth. More specifically, we generated models with three different nucleation locations; 1) ~50km north of the CP; 2) ~50km south of the CP and 3) in the CP. We vary the initial traction of the system using the fault strength parameter $S = \frac{\tau_{yield} - \tau_{initial}}{\tau_{initial} - \tau_{final}}$ (Andrews et al., 1976), using values of S=1 and S=2. Lower S values indicate a system more favorable to rupture while higher S values indicate the opposite. Finally, for some of our experiments we repeated the simulations with locking depths of 10km instead of the original fixed at 15km. The combination of different simulation parameters (e.g. nucleation location, pre-stress level and locking depth) for the

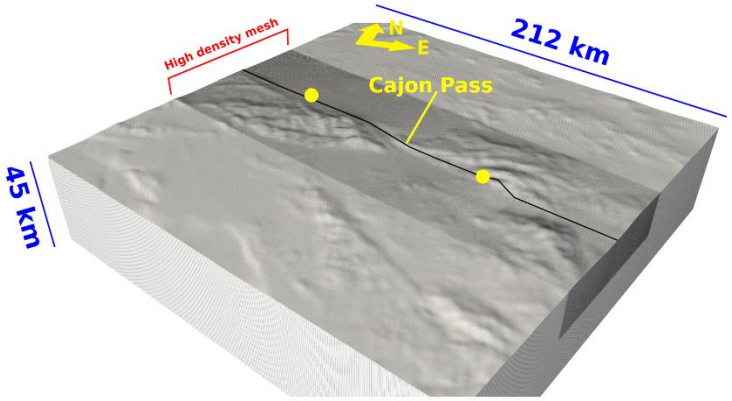

Figure 2. Finite element mesh of Southern California with topography. *The San Andreas fault passes through the Cajon Pass. Our mesh reproduces the asymmetric disposition of the mountains with respect to the fault line (black line). Note: the density of the mesh is higher in the volume surrounding the fault interface and the mountain ranges. The yellow circles show the nucleation locations (south and north of the Cajon Pass) in our numerical simulations.*

topographic and flat cases generated over 20 models. However, due to space limitations, here we show only a subset of our current results that we believe are most relevant for this report.

2.1 Normal stress variations

The most striking result is the observation of normal stress changes induced by the presence of topography. Here we present a description of this effect based on experiments we ran this past year. The geometry of the SSAF (from UCERF3) implemented in our models is vertical across its entire length, but with variations in strike. Normal stress does not change along vertical planar faults in a half-space because of the symmetry of the displacement across the fault interface.

However, variations in normal stress are expected as a result of the changes in fault strike (bending) and are independent from the topographic effects. The results presented in **Figure 3** show that there is an additional source of normal stress change: the topography. **[Please use the map in Figure 1 to locate the observation points (time steps "1" and "2" inside the green and red circles)] Figure 3** shows time snapshots of normal stress changes for two different nucleation scenarios: south of the CP (**Figure 3A** to **3D**) and north of the CP (**Figure 3E** to **3H**) for both topographic (left panel) and flat models (right panel). In this example *S*=2. In the first case, at t = 9 s, rupture propagates northward and is still to the south of the Pass. Note that in this case the topography (San Bernardino Mountains) lies to the right of the fault line as rupture propagates northward. The comparison between **Figure 3A** (topo) and **Figure 3B** (flat) reveals an intense pattern of normal stress change around the rupture front near the free surface in the topographic model. In particular, the rupture front is preceded by an increase in normal stress (clamping - blue color) and followed by a concentration of decreasing normal stress (unclamping – red color). This difference is highlighted in **Figure 3** by two dashed circles marking the location of the rupture front. When rupture passes the CP (**Figure 3C** and **3D** at t =

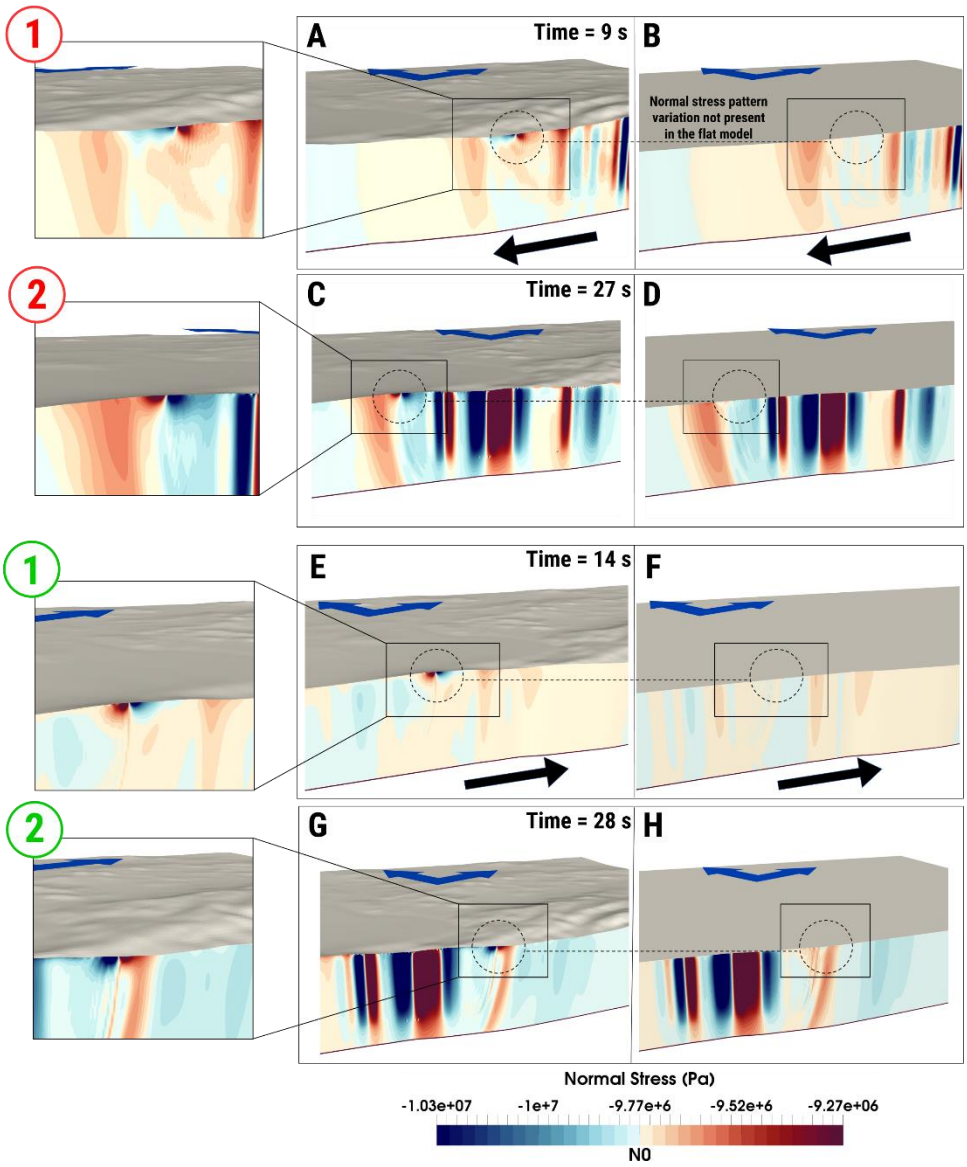

Figure 3. Normal stress variations in the SSAF during northward and southward rupture propagation. *Panels (A) to (D) show experiments with nucleation south of the Cajon Pass – northward propagation. (A) and (B) show the normal stress perturbation at t=9 s while rupture is to the south of the Cajon Pass for the topo and flat models respectively. Here the pattern of normal stress at the rupture front is clamping (blue) – unclamping (red). (C) and (D) shows the normal stress perturbation at t=27 s while rupture is to the north of the Cajon Pass. Note the inversion in normal stress pattern at t=27 s, that is now unclamping (red) – clamping (blue). Panels (E) to (H) correspond to experiment with nucleation north of the Cajon Pass – southward propagation. (E) and (F) show the normal stress perturbation at t=14 s while rupture is to the north of the Cajon Pass for the topo and flat models respectively. Here the pattern of normal stress at the rupture front is clamping (blue) – unclamping (red). (G) and (H) shows the normal stress perturbation at t=28 s while rupture is to the south of the Cajon Pass. Note the inversion in normal stress pattern at t=28 s, that is now unclamping (red) – clamping (blue). Note: use the red and green (1) and (2) to locate the observation points in **Figure 1**. The black think arrows in panels (A), (B), (E) and (F) show the direction of rupture. The term N0 in the colorbar indicates the initial normal stress.*

27 s) and the topography lies to the left of the fault (San Gabriels Mountains) the normal stress pattern is inverted. More specifically, the rupture front is now preceded by a concentration of reduced normal stress (unclamping, red color) and followed by clamping (blue color). The second case (**Figure 3E** to **3H**), nucleation north of the CP (southward propagation), confirms our observations from the first case. Most importantly we observe again the inversion of normal stress pattern when rupture passes the CP.

3. Future work (ongoing investigation)

The normal stress changes (due to the topography) although clearly visible during the dynamic rupture experiments, occur simultaneously with the normal stress changes produced by the along-strike variations of the fault geometry. For that reason, is important to separate the two effects and isolate the purely topographic one. To do that, we generated a new synthetic model that is analogous to the topographic asymmetry around the Cajon Pass, has the same mesh properties (e.g. density near the fault) as the original models, and implements a vertical fault plane without along-strike variations in orientation. We used this model to reproduce a rupture scenario with nucleation south of the CP as in the topographic and flat cases. These new results confirm the findings from our initial work. More specifically, without the confounding variable of fault bends, we observe even more clearly the normal stress changes near the rupture front, with the same pattern as in the case with the realistic topography and fault structure. We are currently working on the analysis of the synthetic models and the comparison with the original results.

4. Implications of our results.

Based on the results from our current work, it appears that the Cajon Pass EQ gate marks a transtion for rupture behavior. We observe normal stress changes associated with the presence of topography and the inversion of normal stress pattern is observed on both scenarios with nucleation locations south and north of the CP. The final goal of our work is to understand if topography and more specifically the asymmetric disposition of the mountains around the CP generates favorable or non-favorable conditions for rupture across the pass. Furthermore, how this effect depends on the direction of rupture propagation and the potential implications for the interpretation of historical events on the SSAF.

5. Intellectual merit

Our work is relevant for at least three major areas of SCEC research. First, the collective effort to study and understand the Cajon Pass Earthquake Gate as a key area for the development of future large events in Southern California. Second, implementing and understanding the effects of realistic features in dynamic rupture models (4a, 4e). For example, in the specific case of southern California, the asymmetric disposition of the San Bernardino and San Gabriels Mountains around the Cajon Pass and the feedback between topography and the rupture front. Third, combining advanced numerical models and HPC to investigate and better understand earthquake rupture phenomena. This activity presented new numerical observations of topography induced rupture effects based on a "bi-topography" interface.

References Cited

Andrews D.J, (1976), Rupture propagation with finite stress in antiplane strain, J. Geophys. Res. Solid Earth, 81, 3575-3582

Barall, M., (2009). A grid-doubling technique for calculating dynamic three-dimensional rupture on an earthquake fault, *Geophysical Journal International*, 178, 845-859, doi:10.1111/j.1365-246X.2009.04190.x.

Bouchon, M., Schultz, C.A. & Toksöz, M.N., 1996. Effect of three-dimensional topography on seismic motion, *Journal of Geophysical Research,* 101**,** 5835-5846.

Bouchon, M., 1973. Effect of topography on surface motion, *Bulletin of the Seismological Society of America,* 63**,** 615-632.

Ely, G.P., Day, S.M. & Minster, J.-B., 2010. Dyanamic rupture models for the southern San Andreas fault, *Bulletin of the Seismological Society of America,* 100**,** 131-150.

Field, E. H., et al., 2013, Uniform California Earthquake Rupture Forecast, version 3 (UCERF3)—The time-independent model, Bull. Seism. Soc. Am, Vol. 104, No. 3, pp. 1122–1180, doi: 10.1785/0120130164

Geli, L., Bard, P.-Y. & Jullien, B., 1988. The effect of topography on earthquake ground motion: a review and new results, *Bulletin of the Seismological Society of America,* 78**,** 42-63.

Kyriakopoulos, C., Oglesby, D.D., Funning, G.J. & Ryan, K.J., 2017. Dynamic rupture modeling of the M7.2 2010 El Mayor-Cucapah earthquake: Comparison with a geodetic model, *Journal of Geophysical Research,* 122**,** 10,263-210,279.

Ma, S., Archuleta, R.J. & Page, M.T., 2007. Effects of large-scale surface topography on ground motions, as demonstrated by a study of the San Gabriel Mountains, Los Angeles, California, *Bulletin of the Seismological Society of America,* 97**,** 2066-2079, doi:2010.1785/0120070040.

Trifunac, M.D., 1973. Scattering of plane SH waves by a semi-circular canyon, *Earthquake Engineering and Structural Dynamics,* 1**,** 267-281.

Wong, H.L., 1982. Effect of surface topography on the diffraction of P, SV, and Rayleigh waves, *Bulletin of the Seismological Society of America,* 72**,** 1167-1183.

Zhang, Z., Xu, J. & Chen, X., 2015. The supershear effect of topography on rupture dynamics, *Geophysical Research Letters,* 43**,** 1457-1463.